NEW CONCEPT OF A HYBRID AMPLIFIER FOR DRIVING PIEZOELECTRIC ACTUATORS

Christoph Stiebel, Hartmut Janocha

Saarland University, Laboratory for Process Automation (LPA), Saarbrücken, Germany

Abstract: This paper describes a new concept of an amplifier for piezoelectric actuators, which combines the high efficiency of a switching amplifier with the output signal accuracy of an analogue amplifier. This so-called *hybrid amplifier* includes a bidirectional switching voltage source and an analogue final stage. The description of the control unit for the switching power supply with its unconventional structure form the main focus of this paper, simulated and measured output signals from the amplifier as implemented are included.

Keywords: piezoelectric actuators, driving electronics, amplifier, energy recovery, high efficiency, mechatronic system

1. INTRODUCTION

The use of piezoelectric actuators as small, highly dynamic drives within mechatronic systems has up to now been limited by the driving amplifier. On the one hand there are small transducers with a high power density, strong achievable forces and short mechanical reaction times. On the other hand are bulky, inefficient amplifiers that restrict the system dynamics to keep the power losses within tolerable limits. The reason for these power losses (which increase proportionally with the operating frequency) is the large energy requirement necessary to build up the electrical field in the transducer. Typically 70 % of the applied field energy is dissipated into heat in the power stage during the discharging process (Vetter and Reuss, 1996).

A high efficiency of the driving electronics — the basic condition for its miniaturization — necessitates the electronics to build up the field energy with minimal power losses, as well as to recover the field energy stored in the transducer in case of field reduction. Both requirements can only be achieved by a switching amplifier.

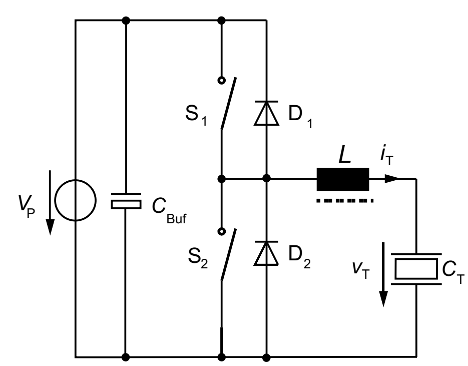

Fig. 1. Basic configuration of a bidirectional switching amplifier (Janocha and Stiebel, 1998)

2. CLASSICAL BIDIRECTIONAL SWITCHING AMPLIFIER

Figure 1 shows the basic configuration of a classical bidirectional switching amplifier, which is able to build up the field energy in the transducer with minimal power losses and to recover the stored field energy in case of field reduction.

A primary voltage supply supplies the circuit with the constant voltage V_P. Two switches S_1 and

S_2 can either connect this voltage with the LC_T-series resonant circuit or short it.

To charge the transducer C_T switch S_1 must be closed. The current i_T now flows from the supply V_P via S_1 and the inductor L to C_T and the voltage v_T rises. At time t_{off} S_1 is opened but because of the inductance L a freewheel current through the diode D_2 will continue to charge the transducer until time t_{end}, when L is demagnetized and the diode cuts off.

Figure 2 shows the voltage and current transients for a voltage jump from 100 V to 150 V.

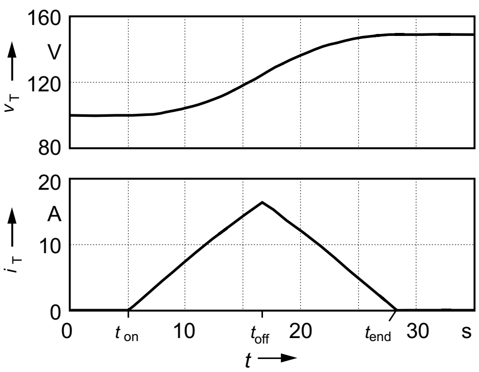

Fig. 2. Voltage and current transients for one switching cycle (Janocha and Stiebel, 1998)

To discharge the transducer, S_2 is closed and the transducer stores a portion of its field energy in the inductance L. Before the desired voltage v_T at the transducer is reached, S_2 has to be opened (at t_{off}). The freewheel current through the diode D_1 now allows the energy to return to the primary supply (energy recovery).

3. SWITCHING AMPLIFIER WITH SMART SWITCHING

In (Janocha and Stiebel, 1998) a controller concept is presented, that transfers in every switching cycle exactly that portion of energy necessary to achieve a desired voltage at the transducer. Thus unnecessary switching cycles — which merely heat the transducer and semiconductor components — can be avoided.

By the explicit evaluation of the differential equation of the converter system in every switching configuration the exact time t_{off} needed to achieve any desired voltage across the transducer in one switching cycle can be calculated. The result is:

$$t_{off} = \sqrt{L \cdot C_T} \left| \arcsin\left(\frac{K_1}{K_2}\right) - \frac{\pi}{2} \right| \qquad (1)$$

with K_1 and K_2 different for charging and discharging and only dependent on the actual and desired voltage at the transducer. To achieve a precise switching on the order of several hundred kilohertz, which is necessary for excellent output signals, this compution has to be done in less than a microsecond. An economical method to fulfill this hard time limit is to tabulate the switching times for all combinations of the actual and the desired value (v_{in}) of the transducer voltage in a $2 \cdot 64$ kByte = 128 kByte EPROM memory. During operation this ROM table is directly addressed by the output of two fast A/D converters sampling the respective system variables; the output signal of the memory is the desired time t_{off}. By modifying the ROM table, which follows directly from equation (2), current limiting can be implemented without current sensing.

Figure 3 shows the block diagram of the implemented switching amplifier with smart (precise) switching.

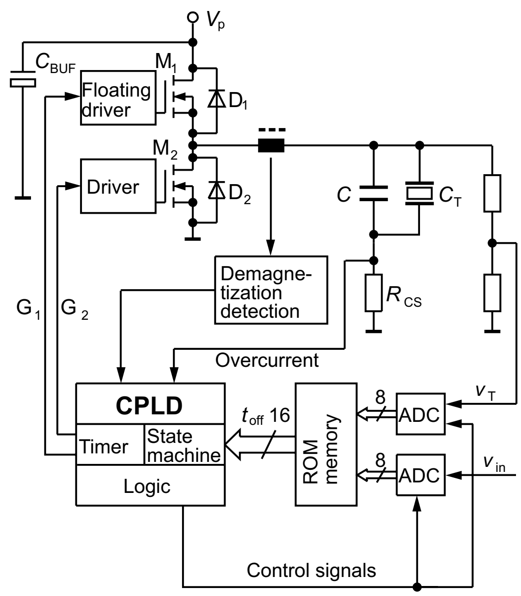

Fig. 3. Block diagram of the implemented switching amplifier with smart switching (Janocha and Stiebel, 1998)

The whole control logic of the amplifier is implemented in a single low-cost CPLD (Complex Programmable Logic Device). Every time the current through the inductor is zero, the demagnetization detection starts a new operation cycle. Each operation cycle consists of the following steps: sampling v_{in} and v_T, converting to digital, addressing the memory directly with the digital values, loading the switching time t_{off} from the memory into the CPLD, starting the timer with the value t_{off} and switching the relevant MOSFET for the duration of the time t_{off}. This leads to a free-oscillating system which adapts its switching frequency to the requirements of the input signal. The overcurrent detection is merely an additional security function and is not necessary for normal operation.

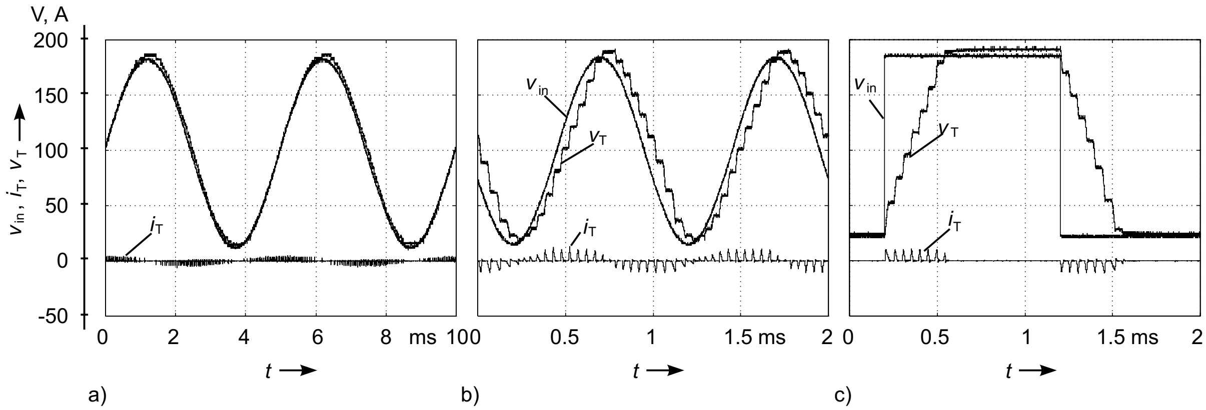

Fig. 4. Measured output signals of an amplifier implemented according to Figure 3 (Janocha and Stiebel, 1998)
a) 200 Hz sinusodial signal b) 1 kHz sinusodial signal c) 500 Hz rectangular signal

Figure 4 shows some characteristic transient plots of the implemented amplifier with smart switching. The output signal accuracy is excellent for a switching amplifier. In Figure 4a the plots for v_{in} and v_{T} are hard to distinguish. In case of higher signal frequencies (Figure 4b) the working principle and the special features of the amplifier become obvious. The output signal v_{T} always lags one switching cycle behind the input v_{in}. A new switching cycle can only be started if the inductor current i_{T} zero. On examining the 500 Hz rectangular signal (Figure 4b) additional features can be noticed. The cycle-by-cycle current limit (12 A), implemented directly in the switching table, causes the voltage to rise in several steps. With the last step the desired transducer voltage is exactly reached and the amplifier stops switching. Since the transducer capacitance will never be overloaded additional switching cycles to correct the output voltage will not occur.

All these features would be considerably more difficult to achieve with traditional pulse width modulated switching amplifiers.

To sum up: The switching amplifier with smart switching has a high efficiency and produces excellent voltage transients at the transducer. In particular it seems to be the ideal driving electronics for the highly dynamic large-signal operation of piezoelectric transducers. The reason for further investigations in piezoelectric driving electronics becomes clearer upon viewing on Figure 2 and Figure 4 more closely. Despite the switching, the voltage transient from 100 V to 150 V is relatively smooth, however the current transients shows sharp peaks. The influence of such peaks in the charge current on a piezoelectric ceramic on its mechanical stress is investigated in (Stiebel *et al.*, 1999). Furthermore a circuit, consisting of a switching power supply and an analogue final stage, which avoids these current transients is presented there.

4. COMBINATION OF A SWITCHING AND AN ANALOGUE AMPLIFIER TO A HYBRID AMPLIFIER

Figure 5 shows the combination of a bidirectional switching amplifier and an analogue final stage to form a hybrid amplifier.

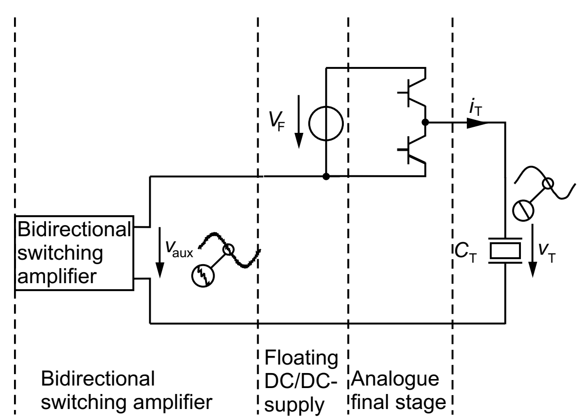

Fig. 5. Hybrid amplifier

The charging and discharging occurs as in a simple analogue amplifier with a high precision through the analogue final stage. The power supply of the analogue final stage is as opposed to an analogue amplifier, not the maximum transducer voltage (200 . . . 1000 V), but a much smaller voltage $V_{\mathrm{F}} = 20 \ldots 40$ V. Therefore the power losses remain small, although the total transducer current flows through the analogue final stage. The proper function of the circuit requires that the output voltage v_{aux} of the bidirectional switching amplifier tracks exactly the voltage v_{T} across the transducer.

$$v_{\mathrm{aux}} \leq v_{\mathrm{T}} \leq v_{\mathrm{aux}} + V_{\mathrm{F}} \qquad (2)$$

If eq. (2) is not satisfied the analogue final stage cannot work and an analogue charging/discharging of the transducer is no longer possible. In this case, the ripples would come through the analogue stage to the transducer.

5. BIDIRECTIONAL SWITCHING AMPLIFIER AS A PART OF A HYBRID AMPLIFIER

For the bidirectional switching amplifier in figure 5 the circuit in figure 1 could be used, if the transducer capacitance is replaced by a small fixed capacitor C_{aux}. Because the energy stored in this capacitor has also to be transfered from the switching amplifier the capacitance of C_{aux} should be as small as possible. With a small capacitance the influence of the analogue final stage and the transducer on the voltage v_{aux} cannot be neglected. This influence can be modelled as a variable current source i_0 in parallel with C_{aux}, because during one switching cycle the charge current for the transducer remains constant. For smart switching this current has also to be measured and considered for the calculation of the switching time t_{off}. Doing so the ROM table must be expanded by one dimension, which means $2 \cdot 2^{24}$ Byte $= 32$ MByte instead of 128 kByte. Today 32 MByte ROM memory are only available as compact flash PCMCIA cards which are still expensive and cannot be programmed with a standard EPROM programmer.

Consequently an other configuration shown in Figure 6 was chosen, which allows again a two-dimensional ROM addressing.

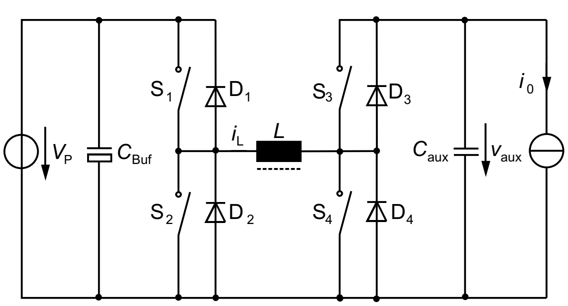

Fig. 6. Bidirectional switching stage suited for a hybrid amplifier

In Figure 6 the analogue final stage and the transducer are also modelled as a variable current source i_0.

The addition of switches S_3 and S_4 results in current paths for the inductor current that do not include C_{aux}. Over these paths the inductor current can flow without changing the voltage v_{aux}.

To build up the voltage v_{aux} across the capacitor C_{aux} switches S_1 and S_4 have to be closed. Now the inductor current rises according to

$$i_{\mathrm{L}}(t) = \frac{V_{\mathrm{P}} \cdot t}{L} \quad \text{with} \quad V_{\mathrm{P}} = 800 \ldots 1000 \text{ V}. \quad (3)$$

During this phase the inductor current has still no influence on the voltage v_{aux}. When the inductor current has reached the value $i_{\mathrm{L\,max}}$ at time t_{off} the switches are opened. Now the inductor gives its stored energy $E_{\mathrm{L}}(i_{\mathrm{L\,max}}) = 1/2 \cdot L \cdot i_{\mathrm{L\,max}}^2$ through the diodes D_2 and D_3 to capacitor C_{aux} and voltage v_{aux} rises. By changing the switching time t_{off} the voltage jump at the output of the switching stage Δv_{aux} can be controlled.

To lower the voltage v_{aux} the switches S_2 and S_3 are closed and the capacitor C_{aux} stores a portion of its field energy in the inductor L, so the voltage v_{aux} falls. When the switches open the falling of the output voltage stops without a time constant. Now inductor L allows the stored energy to return to the primary supply (buffer capacitor C_{Buf}).

6. CONTROL OF THE BIDIREKTIONAL SWITCHING AMPLIFIER IN A HYBRID AMPLIFIER CONCEPT

Figure 7 shows the power stage and the controller for the bidirectional switching amplifier in a hybrid amplifier configuration. As mentioned above the principle of the hybrid amplifier requires that the voltage at the auxiliary capacitor C_{aux} always tracks the transducer voltage v_{T} with a difference of 10 to 20 V without any time lagging or overshooting. To achieve this feature smart switching has to be implemented for the power stage from Figure 6.

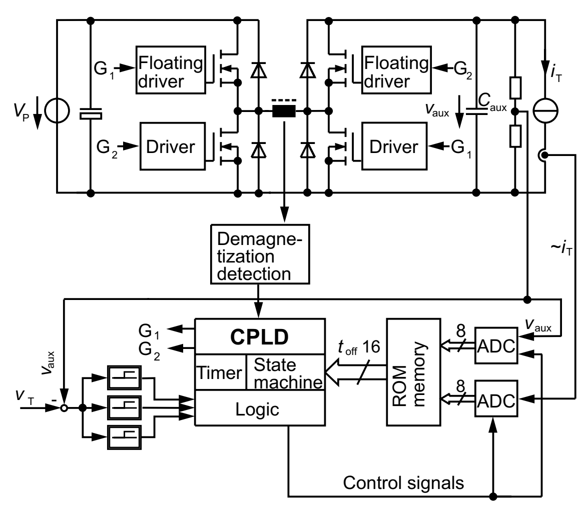

Fig. 7. Controller for the bidirectional switching amplifier in a hybrid amplifier configuration

The central control element is also a freely programmable low-cost CPLD. It includes a logic to

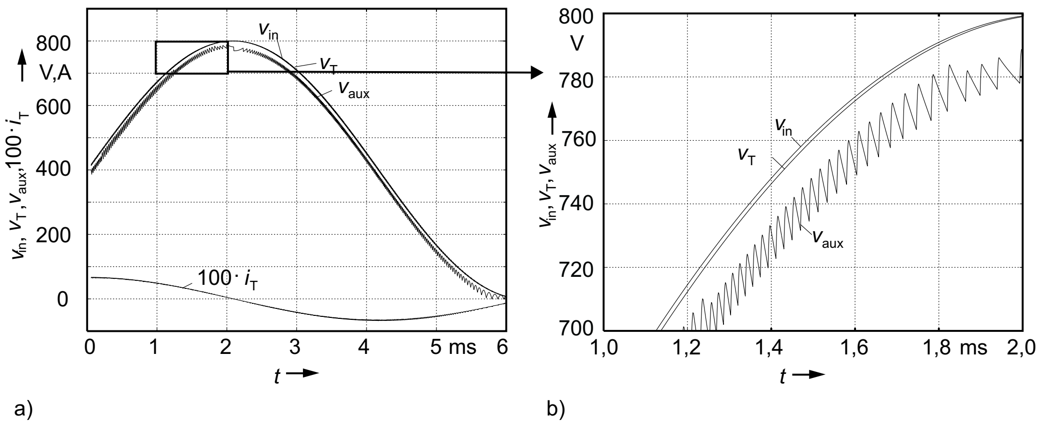

Fig. 8. Simulation results of the hybrid amplifier

evaluate diverse comparator outputs, a state machine for controlling the sequencing and a counter to dose the switching times of the transistors.

The condition to initiate a new switching cycle is always that the inductor is demagnetized and that the difference of the transducer voltage v_T and the voltage at the auxiliary capacitor v_aux exceed or fall below a certain limit.

If the difference is too small, C_aux has to be discharged. The CPLD is informed of this state by a comparator and the respective MOSFETs are turned on (signal G_2) until the voltage difference is correct (information from another comparator). After opening the switches the discharging process stops without a time constant and the inductor feeds the stored field energy back to the buffer capacitor C_Buf.

In case the voltage difference is too high a charging cycle gets initiated. This cycle is more complex than a discharging cycle. As mentioned above the voltage jump Δv_aux at the output of the switching stage is controllable by changing the time t_off when switches S_1 and S_4 are opened. By using the energy balance equation and the differential equations of the charging process the exact time t_off to reach a certain voltage step Δv_aux can be calculated. The switching time is a nonlinear function dependent on Δv_aux, the instantaneous output voltage $v_\mathrm{aux}(0)$ ($t = 0$ when switches close) and the instantaneous output current i_0. To control the voltage jump Δv_aux the nonlinear function $t_\mathrm{off}(\Delta v_\mathrm{aux},\ v_\mathrm{aux}(0),\ i_0)$ has to be computed in less than a microsecond because the small capacitor C_aux is permanently discharged through i_0. If the control unit works with constant voltage jumps for instance $\Delta v_\mathrm{aux} = 10$ V, $t_\mathrm{off}(v_\mathrm{aux}(0),\ i_0)$ has only two changing variables $v_\mathrm{aux}(0)$ and i_0. This function can be tabled and stored in a $2 \cdot 64$ kByte EPROM memory, which is directly addressed by two fast 8-Bit A/D converters sampling the values of $v_\mathrm{aux}(0)$ and i_0. Further on the control scheme is similar to section 3.

Doing so an exact tracking of the voltage v_aux is always possible.

7. SIMULATION RESULTS

Figure 8 shows simulation results of a hybrid amplifier of 0 . . . 800 V output voltage with a maximum transducer current of ±750 mA driving a 2.2 μF piezoelectric transducer. The capacitance of the auxiliary capacitor is only 400 nF. In Figure 8a the desired value of the transducer voltage v_in, the actual transducer voltage v_T as well as the voltage v_aux at the auxiliary capacitor C_aux and the charge current of the transducer are plotted. The voltage v_aux tracks exactly the voltage at the transducer with a difference of 10 to 20 V without any time lagging and overshooting. So the pre-condition for the faultless function of the analogue final stage, removing all ripples form the transducer voltage v_T and the transducer current i_T, is always guaranteed. The smooth plots of v_T and i_T are proof of the proper function of the analogue final stage and the total hybrid amplifier concept.

Figure 8b is a zoomed illustration of the area from 700 . . . 800 V. Now the switching ripples at the voltage v_aux are better to detect as well as a small deviation of the desired and the actual voltage at the transducer. Switching ripples at the transducer voltage and in the charging current are not visible even under a higher resolution.

8. MEASUREMENT RESULTS OF THE FIRST PROTOTYPE

In Figure 9 measurement results from the first prototype with a smaller supply voltage (200 V) are presented. A smaller supply voltage was chosen for the first prototype to lessen the problems associated with the isolated gate drives necessary for switches S_1 and S_4. The measurements (Figure 9a) verify that the hybrid amplifier is more than

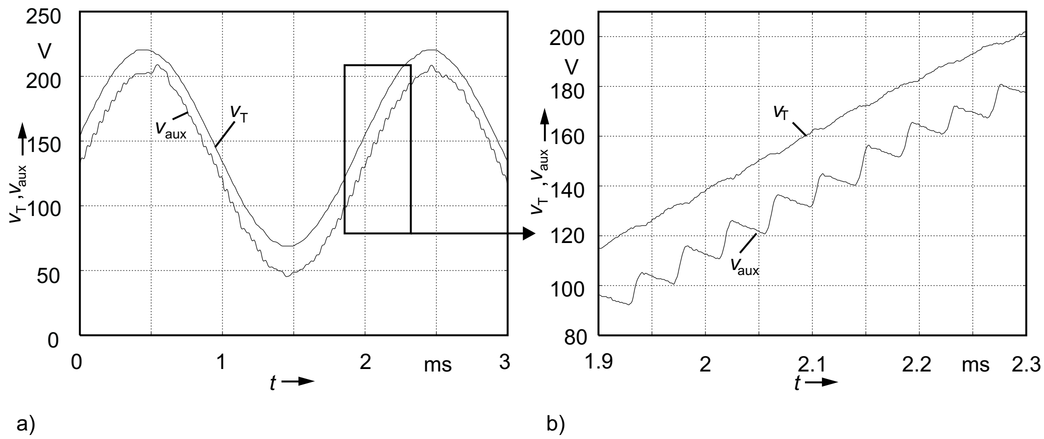

Fig. 9. Measuring results of the first implementation of a hybrid amplifier

just an academic concept. On the other hand they manifest tasks to solve in the future, such as increasing the supply and output voltage and improving the analogue final stage to totally damp the voltage steps (Figure 9b).

9. CONCLUSION

In this paper starting from a switching amplifier for piezoelectric transducers with nearly ideal output voltage transients a new amplifier concept is presented. The so-called hybrid amplifier consists of a switching voltage supply and an analogue final stage. The hybrid amplifier fulfills all essential requirements of an ideal driving electronics for piezoelectric transducers, such as:

- high efficiency in highly dynamic large-signal operation (switching amplifier),
- high output signal accuracy (analogue amplifier) and
- "stress free" driving of piezoelectric transducers without any discontinuities in the charge current (analogue amplifier).

The main problem of this concept, the exact tracking of the transducer voltage with a switching amplifier, has been solved with an unconventional control unit.

10. REFERENCES

Janocha, H. and C. Stiebel (1998). New approach to a switching amplifier for piezoelectric actuators. In: *Proc. of the 6th International Conf. on New Actuators*. Messe Bremen GmbH. pp. 189–192. Bremen, Germany.

Stiebel, C., T. Würtz and H. Janocha (1999). Analogverstärker mit Energierückgewinnung zum Ansteuern von piezoelektrischen Aktoren. In: *SPS/IPC/DRIVES; Elektrische Automatisierungstechnik – Systeme und Komponenten*. MESAGO. pp. 693–702. Nürnberg.

Vetter, T. and H.C. Reuss (1996). Modelling of piezoactuators and newly developed control unit for inside–automotive applications. In: *Proc. of the 5th International Conf. on New Actuators*. AXON Technologie Consult GmbH. pp. 187–192. Bremen, Germany.